

Deltahedral Germanium Clusters: Insertion of Transition-Metal Atoms and Addition of Organometallic Fragments

Jose M. Goicoechea and Slavi C. Sevov*

Contribution from the Department of Chemistry and Biochemistry, University of Notre Dame, Notre Dame, Indiana, 46556

Received December 21, 2005; E-mail: ssevov@nd.edu

Abstract: Reactions of nine-atom deltahedral clusters of germanium with Ni(COD)₂ and/or Ni(PPh₃)₂(CO)₂ in ethylenediamine yielded the Ni-centered heteroatomic 10-atom clusters [Ni@(Ge₉Ni-CO)]²⁻ and [Ni@(Ge₉Ni-en)]³⁻, as well as the empty 10-atom heteroatomic cluster [Ge₉Ni-CO]³⁻. A ligand exchange reaction between [Ni@(Ge₉Ni-CO)]²⁻ and potassium phenylacetylide produced the organically functionalized species [Ni@(Ge₉Ni-CCPh)]³⁻. The empty cluster [Ge₉Ni-CO]³⁻ is a bicapped square antiprism where one of the capping vertexes is the nickel atom. The other three clusters are tricapped trigonal prisms where an additional 10th vertex of monoligated nickel caps a triangular base of the trigonal prism. As a result of this, that base opens up, and the distances within it become nonbonding. This ensures that all atoms of the cluster are equidistant from the central nickel atom, i.e., the cluster is very close to spherical. All species were structurally characterized in crystalline compounds with [K-(2,2,2-crypt)]⁺ counteranions. They were also characterized in solution by mass spectrometry, IR, and ¹³C NMR.

Introduction

Until recently nine-atom deltahedral clusters of group 14 were of interest simply for their shape, bonding, overall negative charges, and somewhat challenging synthesis. Subsequently, numerous publications dealt with synthetic approaches, use of different counteranions, and discussion of the geometries of the resulting clusters.¹ Much less attention was paid to their reactivity while their redox chemistry remained largely ignored. Perhaps the major reason for this omission was the common belief that these species were so highly reduced that reaction with most common reagents would lead to their decomposition. For a long time, the only reported reaction involving such clusters was ligand-exchange where a labile ligand of an organometallic compound was replaced with a cluster. For example, L in LM(CO)₃ where M = Cr, Mo, or W and L = mesitylene, cycloheptatriene, or toluene can be replaced by Sn₉⁴⁻ or Pb₉⁴⁻ to produce [Sn₉M(CO)₃]⁴⁻ and [Pb₉M(CO)₃]⁴⁻, respectively.² The resulting 10-atom clusters are bicapped square antiprisms that carry 22 cluster-bonding electrons and, therefore, qualify as *closo*-clusters. (Each Sn- or Pb-atom contributes two bonding electrons while the other two electrons form a lone pair. The capping M(CO)₃ fragment has three empty orbitals and does not provide bonding electrons.)

More recently, we and others have shown that the clusters, specifically those of germanium, can undergo redox reactions

and can bond to each other to form dimers, [Ge₉-Ge₉]^{6-,3} trimers, [Ge₉=Ge₉=Ge₉]^{6-,4} tetramers, [Ge₉=Ge₉=Ge₉=Ge₉]^{8-,5} and infinite chains, ∞[-(Ge₉²⁻)-].⁶ Furthermore, we have also shown that they can be functionalized by a variety of R groups such as -SbPh₂, -BiPh₂, -GeMe₃, -GePh₃, -SnMe₃, -SnPh₃, -Ph, etc., and form species such as [Ge₉-R]³⁻, [R-Ge₉-R]²⁻, and [R-Ge₉-Ge₉-R].^{4-,7} In addition, there was also an isolated report of a nickel-centered cluster of nine germanium and one ligated nickel atom, [Ni@(Ge₉Ni-PPh₃)]²⁻ (**6**), made by a reaction of germanium clusters with Ni(PPh₃)₂(CO)₂ at somewhat elevated temperatures (in order to drive off CO).⁸ Until very recently there were no other reports of such reactions involving germanium clusters, although similar reactions with tin and lead clusters were studied and produced the analogous [Ni@(Sn₉Ni-CO)]³⁻ and [Pt@(Sn₉Pt-PPh₃)]²⁻ species as well as the novel [Ni@Pb₁₀]²⁻ and [Pt@Pb₁₂]²⁻ clusters.⁹⁻¹¹ We were intrigued specifically by the germanium species due to our

- (1) Reviews: (a) Corbett, J. D. *Chem. Rev.* **1985**, 85, 383. (b) Corbett, J. D. *Struct. Bonding* **1997**, 87, 157. (c) Corbett, J. D. *Angew. Chem., Int. Ed.* **2000**, 39, 670. (d) Fässler, T. F. *Coord. Chem. Rev.* **2001**, 215, 377.
 (2) (a) Eichhorn B. W.; Haushalter, R. C.; Pennington, W. T. *J. Am. Chem. Soc.* **1988**, 110, 8704. (b) Eichhorn, B. W.; Haushalter, R. C. *Chem. Commun.* **1990**, 937. (c) Kesanli, B.; Fettinger, J.; Eichhorn, B. *Chem. Eur. J.* **2001**, 7, 5277. (d) Campbell, J.; Mercier, H. P. A.; Holger, F.; Santry, D.; Dixon, D. A.; Schrobilgen, G. J. *Inorg. Chem.* **2002**, 41, 86.

- (3) (a) Xu, L.; Sevov, S. C. *J. Am. Chem. Soc.* **1999**, 121, 9245. (b) Hauptmann, R.; Fässler, T. F. *Z. Anorg. Allg. Chem.* **2003**, 629, 2266.
 (4) (a) Ugrinov, A.; Sevov, S. C. *J. Am. Chem. Soc.* **2002**, 124, 10990. (b) Yong, L.; Hoffmann, S. D.; Fässler, T. F. *Z. Anorg. Allg. Chem.* **2005**, 631, 1149.
 (5) (a) Ugrinov, A.; Sevov, S. C. *Inorg. Chem.* **2003**, 42, 5789. (b) Yong, L.; Hoffmann, S. D.; Fässler, T. F. *Z. Anorg. Allg. Chem.* **2004**, 630, 1977.
 (6) (a) Downie, C.; Tang, Z.; Guloy, A. M. *Angew. Chem., Int. Ed.* **2000**, 39, 338. (b) Downie, C.; Mao, J.-G.; Parmer, H.; Guloy, A. M. *Inorg. Chem.* **2004**, 43, 1992. (c) Ugrinov, A.; Sevov, S. C. *Compt. Rend. Chim.* **2005**, 8, 1878.
 (7) (a) Ugrinov, A.; Sevov, S. C. *J. Am. Chem. Soc.* **2002**, 124, 2442. (b) Ugrinov, A.; Sevov, S. C. *J. Am. Chem. Soc.* **2003**, 125, 14059. (c) Ugrinov, A.; Sevov, S. C. *Chem. Eur. J.* **2004**, 10, 3727.
 (8) Gardner, D. R.; Fettinger, J. C.; Eichhorn, B. W. *Angew. Chem., Int. Ed. Engl.* **1996**, 35, 2852.
 (9) Kesanli, B.; Fettinger, J.; Gardner, D. R.; Eichhorn, B. J. *Am. Chem. Soc.* **2002**, 124, 4779.
 (10) Esenturk, E. N.; Fettinger, J.; Eichhorn, B. W. *Chem. Commun.* **2005**, 247.
 (11) Esenturk, E. N.; Fettinger, J.; Lam, Y.-F.; Eichhorn, B. W. *Angew. Chem., Int. Ed.* **2004**, 43, 2132.

ongoing study of the reactivity of germanium clusters and decided to revive the research conducted nine years ago and explore the reactivity of germanium clusters toward a series of transition metal adducts. This led to the synthesis of the Ni-centered Ge_9 cluster $[\text{Ni}@\text{Ge}_9]^{3-}$ (**5**),¹² an unprecedented species consisting of a linear trimer of nickel enclosed inside two vertex-fused Ge_9 clusters, $[\text{Ni}_3@(\text{Ge}_9)_2]^{4-}$,¹² and the single-cage deltahedron of 18 germanium atoms enclosing a dimer of palladium atoms, $[\text{Pd}_2@(\text{Ge}_9)_2]^{4-}$.¹³ Herein we report the synthesis, structures, and reactivity of a series of NiL-capped Ge_9 clusters, some with and some without an interstitial nickel atom.

Results

Synthesis. The compounds presented here contain four different clusters: an empty Ni(CO)-capped cluster, $[\text{Ge}_9\text{Ni-CO}]^{3-}$ (**1**); a Ni-centered, Ni(CO)-capped cluster, $[\text{Ni}@\text{Ge}_9\text{Ni-CO}]^{2-}$ (**2**); a Ni-centered, Ni(C≡CPh)-capped cluster, $[\text{Ni}@\text{Ge}_9\text{Ni-CCPh}]^{3-}$ (**3**); and a Ni-centered, Ni(en)-capped cluster, $[\text{Ni}@\text{Ge}_9\text{Ni-en}]^{3-}$ (**4**). Clusters **1**, **2**, and **4** were synthesized by reactions of ethylenediamine solution of K_4Ge_9 with $\text{Ni}(\text{COD})_2$, $\text{Ni}(\text{PPh}_3)_2(\text{CO})_2$, or both (COD = cyclooctadiene), while cluster **3** was achieved by ligand-exchange reaction of the ligand in **2** with potassium phenylacetylide.

We have already shown that nine-atom germanium clusters with charges of 2⁻, 3⁻, and 4⁻ exist in equilibria with solvated electrons in their ethylenediamine solutions, i.e., $\text{Ge}_9^{4-} \rightleftharpoons \text{Ge}_9^{3-} + e^- \rightleftharpoons \text{Ge}_9^{2-} + 2e^-$.^{7b,c} In the absence of other reagents, the solvated electrons undergo a very slow reaction resulting in the reduction of the ethylenediamine solvent to amide and hydrogen gas, i.e., $\text{H}_2\text{NCH}_2\text{CH}_2\text{NH}_2 + e^- \rightarrow [\text{HNCH}_2\text{CH}_2\text{NH}_2]^- + 1/2\text{H}_2$.⁹ We have shown that triphenylphosphine acts as a mild oxidizing agent when present in such solutions, i.e., $\text{PPh}_3 + 2e^- \rightarrow \text{PPh}_2^- + \text{Ph}^-$.^{7b} The phenyl anion is a strong base and abstracts a proton from the ethylenediamine to form benzene and an amide. COD may have similar reactivity toward the solvated electrons resulting in double bond cleavage and subsequent formation of anions of high basicity that can deprotonate the ethylenediamine solvent. Thus, the reactions of Ge_9^{n-} with $\text{Ni}(\text{PPh}_3)_2(\text{CO})_2$ and $\text{Ni}(\text{COD})_2$ would favor the less reduced clusters Ge_9^{3-} and Ge_9^{2-} , and this is exactly what is observed in all cases. The reported reaction with $\text{Ni}(\text{PPh}_3)_2(\text{CO})_2$ was carried out at somewhat elevated temperature (40 °C) at which the ligands were apparently stripped off and CO driven completely out of the reaction mixture.⁸ This produced the reported $[\text{Ni}@\text{Ge}_9\text{Ni-PPh}_3]^{2-}$ (**6**) which must have ligated back PPh_3 upon cooling to room temperature during crystallization of the product. When we carried out the same reaction at room temperature, the crystalline product was an empty cluster capped with Ni-CO, i.e., $[\text{Ge}_9\text{Ni-CO}]^{3-}$ (**1**). Apparently, the ligands at the nickel cannot be removed completely at this lower temperature, and as a result of this, the clusters are empty. Also, crystallization in this case was achieved by layering with toluene which dissolves PPh_3 quite well and may have extracted it from the ethylenediamine.

The COD ligand in $\text{Ni}(\text{COD})_2$ is very labile and easily provides free nickel atoms that can center the clusters. Thus, less than 1 equivalent of $\text{Ni}(\text{COD})_2$ per Ge_9 cluster results simply in the reported Ni-centered cluster of $[\text{Ni}@\text{Ge}_9]^{3-}$ (**5**).¹² On the

other hand, increasing the amount of $\text{Ni}(\text{COD})_2$ to above 3 equivalents per cluster leads to a dimer of Ni-centered clusters that are fused via a capping Ni-vertex, $[(\text{Ni}@\text{Ge}_9)\text{Ni}-(\text{Ni}@\text{Ge}_9)]^{4-}$.¹² It was speculated that this dimer formed by fusion of $[\text{Ni}@\text{Ge}_9]^{3-}$ with some sort of Ni-centered NiL-capped cluster $[\text{Ni}@\text{Ge}_9\text{Ni-L}]^{3-}$ with a labile L along a reaction such as $[\text{Ni}@\text{Ge}_9]^{3-} + [\text{Ni}@\text{Ge}_9\text{Ni-L}]^{3-} \rightarrow [(\text{Ni}@\text{Ge}_9)\text{Ni}(\text{Ni}@\text{Ge}_9)]^{4-} + \text{L} + 2e^-$. Cluster **4**, $[\text{Ni}@\text{Ge}_9\text{Ni-en}]^{3-}$, is the most likely to play the role of the cluster with a labile ligand.

Carrying out the two previous reactions in a sequence, i.e., reaction of an ethylenediamine solution of K_4Ge_9 with $\text{Ni}(\text{COD})_2$ followed by reaction of the resulting clusters (**5**) with $\text{Ni}(\text{PPh}_3)_2(\text{CO})_2$ at room temperature, resulted in $[\text{Ni}@\text{Ge}_9\text{Ni-CO}]^{2-}$ (**2**). The first reaction inserts the centering nickel atom, while the second reaction adds the capping Ni-CO fragment.

Finally, reaction of **2** with 2-fold excess of $\text{KC}\equiv\text{CPh}$ results in ligand exchange of CO with $[\text{C}\equiv\text{CPh}]^-$ at the capping nickel atom to form $[\text{Ni}@\text{Ge}_9\text{Ni-C}\equiv\text{CPh}]^{3-}$ (**3**). The reaction was monitored by electrospray mass spectrometry which revealed complete exhaustion of the carbonyl starting material and the appearance of new signals corresponding to the phenylacetylide product. Cluster **3** may also be obtained, albeit in lower yields, by reaction of **2** with phenylacetylene.

Crystal Structures. All clusters were crystallized with $[\text{K}(2,2,2\text{-crypt})]^+$ as counterions by layering ethylenediamine solutions with toluene. The empty cluster $[\text{Ge}_9\text{Ni-CO}]^{3-}$ (**1**) can be described as a bicapped square antiprism where one of the capping atoms is the ligated nickel atom (Figure 1). The cluster has two different orientations that are occupied 81 and 19% (see Supporting Information for a drawing of the two overlapped orientations). The Ge-Ge distances fall in the range 2.520(1)–2.821(1) Å with the shortest ones occurring around 4-bonded atoms while the longest ones correspond to distances between 5-bonded atoms. The Ni-Ge distances fall within 2.384(1)–2.523(2) Å, and the differences between them are due mainly to the substantial deviation of the capped face from a perfect square. The Ni-C and C-O distances, 1.716(9) and 1.17(1) Å, respectively, are quite normal and fall within the corresponding ranges of Ni-C and C-O distances observed

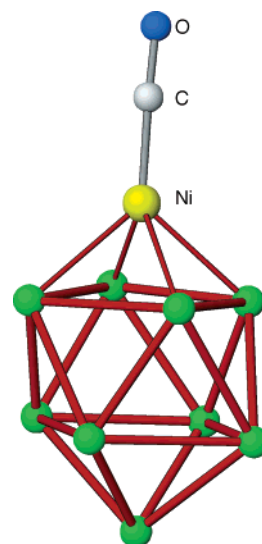


Figure 1. View of $[\text{Ge}_9\text{Ni-CO}]^{3-}$ (**1**) with the shape of a bicapped square antiprism where one of the capping atoms is Ni from the Ni-CO fragment.

(12) Goicoechea, J. M.; Sevov, S. C. *Angew. Chem., Int. Ed.* **2005**, *44*, 2.

(13) Goicoechea, J. M.; Sevov, S. C. *J. Am. Chem. Soc.* **2005**, *127*, 7676.

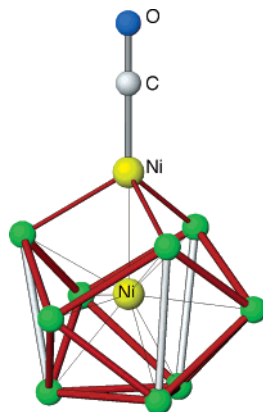


Figure 2. View of $[\text{Ni}@\text{(Ge}_9\text{Ni-CO)}]^{2-}$ (**2**) with the shape of a centered tricapped trigonal prism (vertical) where one of the triangular prismatic bases is additionally capped by the Ni atom from the Ni-CO fragment. The capped base, upper in the figure, opens up and the capping Ni atom becomes part of the cluster.

for crystallographically characterized mononuclear nickel(0) monocarbonyl complexes, 1.60(2)–1.82(1) and 1.12(1)–1.18(2) Å, respectively.^{9,14}

The bicapped square antiprism is a common structural motif for empty nine-atom clusters that are capped by a transition-metal complex fragment as in $[\text{Sn}_9\text{M}(\text{CO})_3]^{4-}$ and $[\text{Pb}_9\text{M}(\text{CO})_3]^{4-}$ for M = Cr, Mo, W.² (It has been shown recently that the $[\text{Sn}_9\text{M}(\text{CO})_3]^{4-}$ species are fluxional and that the $\text{M}(\text{CO})_3$ fragment can also occupy a noncapping position, i.e., a vertex of one of the squares of the square antiprism.)^{2c} There is only one example of this geometry exhibited by a capped cluster that is also centered by a transition metal, $[\text{Ni}@\text{(Sn}_9\text{Ni-CO)}]^{3-}$.⁹ All other centered and capped species are tricapped trigonal prisms in which a triangular prismatic base is additionally capped (and opened) by a transition-metal complex fragment as in $[\text{Ni}@\text{(Ge}_9\text{Ni-PPh}_3)]^{2-}$ (**6**),⁸ $[\text{Pt}@\text{(Sn}_9\text{Pt-PPh}_3)]^{3-}$,⁹ $[\text{Ni}@\text{(Ge}_9\text{Ni-en)}]^{3-}$ (**4**), $[\text{Ni}@\text{(Ge}_9\text{Ni-CCPh)}]^{3-}$ (**3**), and $[\text{Ni}@\text{(Ge}_9\text{Ni-CO)}]^{2-}$ (**2**).

The capped and centered cluster **2**, $[\text{Ni}@\text{(Ge}_9\text{Ni-CO)}]^{2-}$ (Figure 2), has the expected shape discussed above. Furthermore, it also has a three-fold axis along the line defined by Ni(center)–Ni(cap)–C–O (the compound crystallizes in $P6_3/m$). The cluster adopts two different orientations that are mirror images of each other generated by an artificial mirror plane defined by the three Ge-atoms that cap the trigonal prism (see Supporting Information for a drawing of the two orientations overlapped at the position). The distances from the central nickel atom to the open and closed triangular prismatic bases and to the capping atoms are 2.333(3), 2.455(2), and 2.431(1) Å, respectively. This very narrow range of distances together with the Ni–Ni distance of 2.348(4) Å define the cluster as very spherical. The distances from the capping nickel to the three germanium atoms and to the carbon are 2.391(3) and 1.71(2) Å, respectively, and the

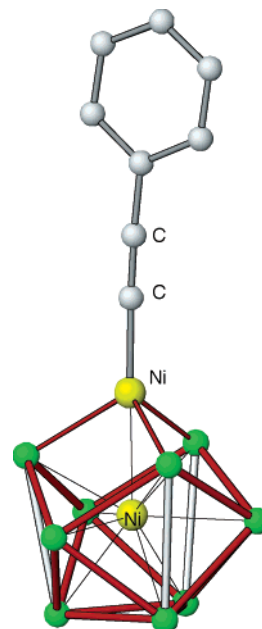


Figure 3. $[\text{Ni}@\text{(Ge}_9\text{Ni-CCPh)}]^{3-}$ (**3**) with the same shape as **2**.

C–O bond distance is 1.16(3) Å. All these distances as well as the range of Ge–Ge distances, 2.626(4)–2.689(3) Å, compare very well with all other clusters of similar shapes as do the elongated prismatic Ge–Ge edges (open vertical bonds in Figure 2) which are significantly longer, 3.070(3) Å.

The shape of cluster **3**, $[\text{Ni}@\text{(Ge}_9\text{Ni-CCPh)}]^{3-}$ (Figure 3), is the same as that exhibited by **2**; however, no disorder is observed for this structure. The cluster is also nicely spherical with a very narrow range of distances from the central nickel to the germanium atoms, 2.3523(8)–2.4411(8) Å, and a distance of 2.3820(8) Å to the capping nickel atom which also falls within this range. The Ge–Ge distances are in the range 2.6254(8)–2.7531(8) Å, while the elongated prismatic edges (vertical open bonds in Figure 3), 3.1042(8), 3.1075(7), and 3.1366(8) Å, are longer as is expected. The capping nickel is bonded to the three germanium vertexes at distances of 2.3672(8), 2.3730(8), and 2.3806(8) Å, while the distance to the carbon is 1.848(5) Å. All C–C distances, including the triple bond of 1.224(7) Å, are also within the normal ranges. The angles at the two triple-bonded carbon atoms are 177.3(5) and 176.4(6)°. There are no known examples of crystallographically characterized nickel(0) acetylides, and therefore, nickel(II) compounds were used for comparison purposes. Thus, when compared to the ranges of Ni–C and C≡C distances in the known Ni(II)-CCPh complexes, 1.821(6)–2.022(7) and 1.166(6)–1.218(14) Å, respectively, the Ni–C distance of 1.848(5) Å in **3** is one of the shorter values, while the C≡C distance of 1.224(7) Å in **3** is the longest observed to date. These observations are in agreement with the expected differences due to the lower oxidation state of Ni and the overall negative charge of the cluster.

Finally, cluster **4** (Figure 4a) is also a nickel-centered, tricapped trigonal prism of germanium in which a nickel atom ligated by an ethylenediamine molecule additionally caps a trigonal prismatic base. The weak Ni–N interaction allows for substantial fluctuations of the ligand and results in relatively large thermal ellipsoids for the ethylenediamine atoms. This cluster occupies its position 73.5%, while the remaining share

(14) (a) Charles, S.; Fettingner, J. C.; Bott, S. G.; Eichhorn, B. W. *J. Am. Chem. Soc.* **1996**, *118*, 4713. (b) Goddard, R.; Tsay, Y. H. *Acta Crystallogr.* **1988**, *C44*, 810. (c) Ferguson, G. S.; Wolczanski, P. T. *Organometallics* **1985**, *4*, 1601. (d) Ghilardi, C. A.; Sabatini, A.; Sacconi, L. *Inorg. Chem.* **1976**, *15*, 2763. (e) Ekici, S.; Nieger, M.; Glaum, R.; Niecke, E. *Angew. Chem., Int. Ed.* **2003**, *42*, 435. (f) Grobe, J.; Krummen, N.; Wehmschulte, R.; Krebs, B.; Läge, M. *Z. Anorg. Allg. Chem.* **1994**, *620*, 1645. (g) Fryzuk, M. D.; MacNeil, P. A. *J. Am. Chem. Soc.* **1984**, *106*, 6993. (h) Ahlemann, J. T.; Roesky, H. W.; Murugarell, R.; Parisini, E.; Nolemeyer, M.; Schmidt, H.-G.; Müller, O.; Herbst-Irmer, R.; Markovskii, L. N.; Shermolovich, Y. G. *Chem. Ber.* **1997**, *130*, 113. (i) Rodewald, D.; Sussmilch, F.; Rehder, D. *An. Quim.* **1996**, *92*, 269.

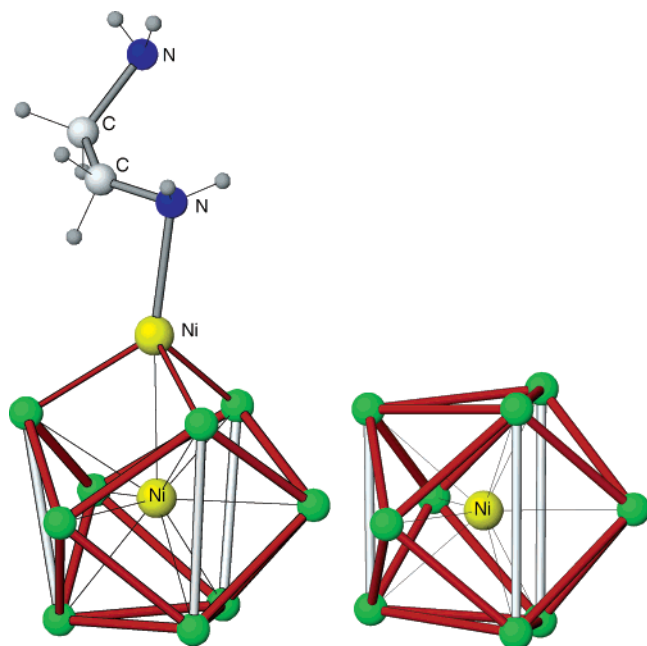


Figure 4. Views of (a) $[\text{Ni}@\text{(Ge}_9\text{Ni-en)}]^{3-}$ (**4**) and (b) $[\text{Ni}@\text{Ge}_9]^{3-}$ (**5**). The two clusters occupy one and the same site with 73.5% occupancy for **4** and 26.5% occupancy for **5**. The only common atom for the two clusters is the centering Ni atom.

is taken by the known $[\text{Ni}@\text{Ge}_9]^{3-}$ (**5**) (Figure 4b). The only common atom for the two clusters is the interstitial nickel atom. The overall different shapes of the clusters lead to different positions for all remaining atoms (see Supporting Information for a drawing of the two clusters overlapped at the position). The ethylenediamine ligand of the capping nickel in $[\text{Ni}@\text{(Ge}_9\text{Ni-en)}]^{3-}$ acts as a noncoordinated solvent molecule when the position is occupied by $[\text{Ni}@\text{Ge}_9]^{3-}$. The central nickel atom in **4** is again nearly equidistant from all cluster atoms, including the capping Ni atom. These distances to the germanium atoms are in the narrow range 2.377(3)–2.435(3) Å, and the Ni–Ni distance is 2.502(1) Å. Again, the latter distance is similar to the Ni–Ge distances only because of the opening of the upper triangular base of the tricapped trigonal prism which allows for the capping nickel atom (the Ni–Ge distances to the open base are 2.316(2), 2.340(2), 2.365(3) Å) to get closer to the center of the cluster. The Ge–Ge distances in the cluster are in the range 2.620(3)–2.782(6) Å while the three elongated prismatic edges, 3.052(5), 3.220(4), and 3.250(4) Å, are noticeably longer than those in **2** and **3**. Overall, all three clusters **2**, **3**, and **4** are very similar to the clusters that form the Ni-

vertex shared dimer of $[(\text{Ni}@\text{Ge}_9)\text{Ni}(\text{Ni}@\text{Ge}_9)]^{4-}$ and to the single cluster $[\text{Ni}@\text{(Ge}_9\text{Ni-PPh}_3)]^{2-}$.^{8,12}

Electrospray Mass Spectrometry. All four compounds are soluble in ethylenediamine and DMF, and their electrospray mass spectra were recorded from such solutions in negative and positive ion modes. In the negative ion mode, as is often the case, the ions are observed either coupled with cations or with a charge that is reduced to 1– during the electrospray process. Due to the multiple isotopes of Ge, Ni, and K, all ions appear as large and very distinctive mass envelopes. The negative ion mode mass spectrum of a solution of **1** reveals a peak corresponding to the $[\text{Ge}_9\text{Ni-CO}]^-$ monoanion (Figure 5a), in addition to peaks arising from Ge₉ generated by the loss of the Ni–CO fragment. The Ni-centered NiL-capped clusters **2**, **3**, and **4** can apparently lose the ligand itself during the ionization process, as all three clusters are accompanied by a peak that corresponds to $[\text{Ni}@\text{(Ge}_9\text{Ni)}]^-$ such as the one pictured in Figure 5b from the mass spectrum of **2**. In addition to this peak, **3** shows a peak that corresponds to $[\text{Ni}@\text{(Ge}_9\text{Ni-CCPh)}]^-$ (Figure 5c). This cluster was also characterized by ¹³C NMR in ethylenediamine solution. The single set of carbon peaks indicates that the cluster is intact in solution, i.e., there are no free CPh[−] anions and $[\text{Ni}@\text{(Ge}_9\text{Ni-en)}]^{2-}$ clusters.

The negative ion spectrum of **2** is the richest, with peaks that correspond to $[\text{Ni}@\text{(Ge}_9\text{Ni)}]^-$, $[\text{Ni}@\text{(Ge}_9\text{Ni-CO)}]^-$, and the ion pairs $\{(\text{K}^+)(\text{Ni}@\text{(Ge}_9\text{Ni-CO)})^{2-}\}^-$, $\{(\text{K}^+)_2(\text{Ni}@\text{(Ge}_9\text{Ni-CO)})^{3-}\}^-$, and $\{(\text{K}(2,2,2\text{-crypt}))^+(\text{Ni}@\text{(Ge}_9\text{Ni-CO)})^{2-}\}^-$ (Figure 6). In addition, the positive-ion spectrum shows a peak that corresponds to the extensively ion-paired species $\{(\text{K}(2,2,2\text{-crypt}))^+\}_3(\text{Ni}@\text{(Ge}_9\text{Ni-CO)})^{2-}\}^+$ (in Supporting Information).

IR Spectroscopy. The IR spectra of the two carbonyl clusters, $[\text{Ge}_9\text{Ni-CO}]^{3-}$ and $[\text{Ni}@\text{(Ge}_9\text{Ni-CO)}]^{2-}$, show C–O absorptions at 1820 and 1930 cm^{-1} , respectively. As can be expected, the lower frequency corresponds to the cluster with the higher overall negative charge. The value of 1820 cm^{-1} is very much in line with the observed stretching frequencies for similar Zintl clusters with a charge of 3–, such as $[\text{Ni}@\text{(Sn}_9\text{Ni-CO)}]^{3-}$ and $[\text{P}_7\text{Ni-CO}]^{3-}$ with bands at 1851 and 1785 cm^{-1} , respectively.^{9,14a} The greater overall cluster charge translates into greater electron density available at the Ni center for π -back-bonding which, in turn, results in a weakening of the CO bond of these species. Tetrahedral Ni(0) monocarbonyl complexes coordinated by tridentate scorpionate-like ligands such as $[\text{MeSi}(\text{OCH}_2\text{PMe}_2)_3]\text{-Ni}(\text{CO})$,^{14f} $[\text{CpZr}(\text{OCH}_2\text{PPh}_2)_3]\text{Ni}(\text{CO})$,^{14c} and $\text{N}[(\text{CH}_2)_2\text{PPh}_2]_3\text{-Ni}(\text{CO})$ ^{14d} have C–O stretching frequencies of 1932, 1905, and 1880 cm^{-1} , respectively, that are also close to those of clusters **1** and **2**. The vibration of the C≡C bond in **3**, 1933 cm^{-1} , is

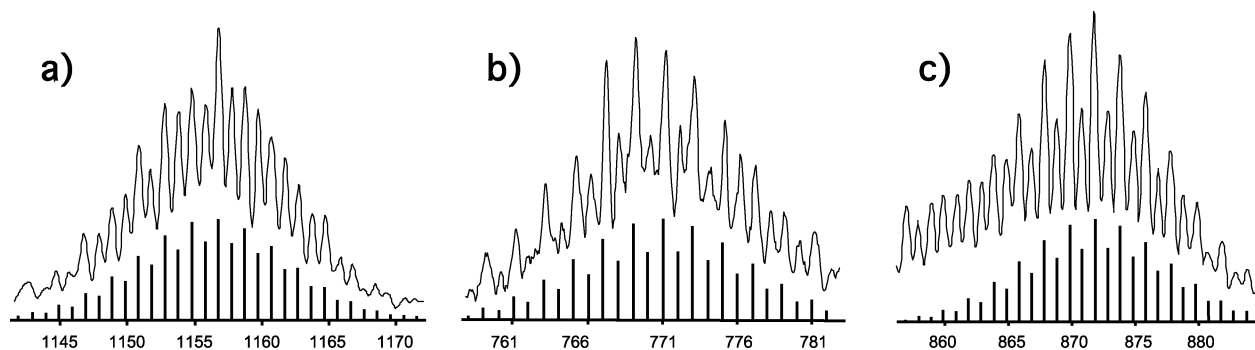


Figure 5. Observed peaks and calculated isotope distributions of (a) $[\text{Ge}_9\text{Ni-CO}]^-$, (b) $[\text{Ni}@\text{(Ge}_9\text{Ni)}]^-$, and (c) $[\text{Ni}@\text{(Ge}_9\text{Ni-CCPh)}]^-$.

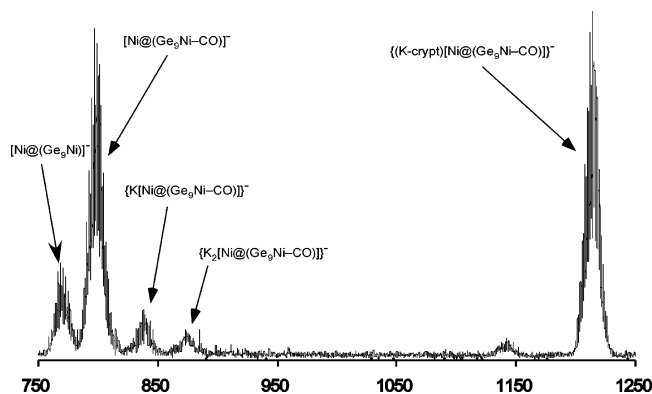


Figure 6. Part of the mass spectrum of (K-crypt)₂[Ni@(Ge₉Ni-CO)]⁻tol in DMF.

noticeably lowered in energy compared to the range of 2081–2160 cm⁻¹ observed for Ni(II) phenylacetylides.¹⁵

Discussion

The fact that Ge₉⁴⁻, Ge₉³⁻, and Ge₉²⁻ coexist in ethylenediamine solutions makes possible the formation of similarly charge-diverse centered and/or capped clusters. It should be mentioned that while Ge₉⁴⁻ and Ge₉³⁻ have been structurally characterized in a number of compounds, Ge₉²⁻ has been elusive. It crystallizes in a compound with [K(2,2,2-crypt)]⁺, but shows such extreme disorder in the resulting hexagonal structure that numerous attempts by us and other groups to refine the structure have been unsuccessful. It is clear, nonetheless, that there are two cations per anion, and this indirectly confirms its existence. Sn₉²⁻ and Pb₉²⁻ show exactly the same problem, while Si₉²⁻ was recently characterized with [K(18-crown-6)]⁺ as a counteranion.¹⁶

To make the discussion easier to follow it is appropriate to briefly go over some general understandings about cluster bonding and electron counting. The deltahedral germanium clusters are directly related to the well-known deltahedral borane clusters B_nH_n^{m-} in the following ways: (a) the bonding within the cluster is achieved by delocalized electrons, (b) a Ge-vertex is isoelectronic with a B-H vertex as both contribute two electrons for cluster bonding, and (c) the numbers of cluster-bonding electrons follow Wade's rules.¹⁷ According to the latter, a *closo*-cluster with *n* vertexes, a *nido*-cluster with *n* - 1 vertexes, and a capped *closo*-cluster with *n* + 1 vertexes require (ideally) the same number of cluster-bonding electrons, 2*n* + 2. Unlike the boranes, however, nine-atom germanium clusters that are electronically intermediate between *closo*- and *nido*-, referred to here as *intermediate* and carrying 2*n* + 1 electrons, are quite stable, i.e., Ge₉³⁻. All these nine-atom clusters are tricapped trigonal prisms with various degrees of elongation of one, two, or all three prismatic edges parallel to the three-fold axis (in the case of one elongated edge the geometry is

equivalent to a monocapped square antiprism). This overall shape is very flexible, and with relatively small elongations or compressions of these edges, the cluster can accommodate 20, 21, or 22 cluster-bonding electrons. This is possible because one of the frontier molecular orbitals which is bonding within the triangular bases of the trigonal prism, but antibonding between them, changes energy dramatically upon these small distortions (orbital drawings are available in ref 7b). This orbital is high in energy and empty for Ge₉²⁻ with 20 cluster-bonding electrons, and the cluster is expected to have a classical trigonal prismatic shape. The orbital becomes stabilized and filled for Ge₉⁴⁻ with 22 electrons, and the cluster exhibits one, two, or three elongated edges. Ge₉³⁻ is an intermediate case in which the HOMO is only partially occupied and the cluster is geometrically similar to Ge₉⁴⁻.

Another important point to keep in mind about clusters in general is that a centering atom provides all of its valence electrons to the delocalized cluster-bonding electrons. This number is zero for nickel, palladium, and platinum because of their closed-shell *d*¹⁰ configuration. Finally, the Ni-CO fragment is isoelectronic with the M(CO)₃ fragment for M = Cr, Mo, W. Both fragments are isolobal with (C-H)³⁺ which means they all have three available but empty frontier orbitals and, therefore, do not provide cluster-bonding electrons.

With this information at hand, we can now view cluster **1** as made of an *intermediate*-Ge₉³⁻ with the shape of a tricapped trigonal prism with one elongated edge, i.e., the special case that is equivalent to a monocapped square antiprism, capped by a Ni-CO fragment (a zero electron donor) at its open face. The shape of the resulting heteroatomic cluster corresponds to a *closo*-borane with 10 vertexes, a bicapped square antiprism of B₁₀H₁₀²⁻. Electronically, however, the latter has 22 bonding electrons, while this number is 21 for **1**. As mentioned above, this shape has been observed for the corresponding Sn₉ and Pb₉ clusters capped with M(CO)₃ for M = Cr, Mo, W, although the resulting [Sn₉M(CO)₃]⁴⁻ and [Pb₉M(CO)₃]⁴⁻ carry 22 electrons instead.² On the other hand, the Ni-centered Ni(CO)-capped cluster of tin, [Ni@(Sn₉Ni-CO)]³⁻, is both isostructural and isoelectronic with **1**.⁹ The calculated HOMO-LUMO gap of 2.42 eV for **1** is understandably somewhat smaller compared to the even-numbered clusters. The half-occupied HOMO and the relatively large HOMO-HOMO(-1) gap of 0.71 eV are clear indications that this cluster should be susceptible to both oxidation and reduction.

Cluster **2**, [Ni@(Ge₉Ni-CO)]²⁻, differs both geometrically and electronically from **1**. The tricapped trigonal prism of Ge₉ in **2** is elongated along all three prismatic edges (open bonds in Figure 2). Furthermore, the Ni-CO fragment in this case caps one of the triangular bases of the trigonal prism. This triangular base opens up to such an extent that the Ge-Ge distances are no longer within the bonding range (not drawn in Figure 2). This justifies the view of the cluster as a tricapped trigonal prism of Ge₉²⁻ with 20 cluster-bonding electrons, i.e., electronically a *closo*-species that is additionally capped by a Ni-CO fragment. According to the electron counting rules mentioned above, such a cluster should remain with 20 electrons, i.e., [Ni@(Ge₉Ni-CO)]²⁻, and this is exactly the case because both the centering nickel and the capping fragment do not donate electrons for cluster bonding. Accordingly, the calculated HOMO-LUMO gap of 2.88 eV is quite large, and this, in a

- (15) (a) Zargarian, D.; Groux, L. F. *Organometallics* **2003**, *22*, 4759. (b) Klein, H.-F.; Zweiner, M.; Petermann, A.; Jung, T.; Cordier, G.; Hammerschmitt, B.; Florker, U.; Haupt, H.-J.; Dartiguenave, Y. *Chem. Ber.* **1994**, *127*, 1569. (c) Berry, J. F.; Cotton, F. A.; Murillo, C. A. *Dalton Trans.* **2003**, 3015. (d) Spofford, W. A.; Carfagna, P. D.; Amma, E. L. *Inorg. Chem.* **1967**, *6*, 1553. (e) Davies, G. R.; Mais, R. H. B.; Owston, P. G. *J. Chem. Soc. A* **1967**, 1750. (f) Whitfall, I. R.; Humphrey, M. G.; Hockless, D. C. R. *Aust. J. Chem.* **1998**, *51*, 219. (g) Walther, D.; Stollenz, M.; Görls, H. *Organometallics* **2001**, *20*, 4221. (h) Wang, R.; Belanger-Gariepy, F.; Zargarian, D. *Organometallics* **1999**, *18*, 5548. (i) Berry, J. F.; Cotton, F. A.; Murillo, C. A.; Roberts, B. K. *Inorg. Chem.* **2004**, *43*, 2277. (16) Goicoechea, J. M.; Sevov, S. C. *Inorg. Chem.* **2005**, *44*, 2654. (17) Wade, K. J. *Adv. Inorg. Chem. Radiochem.* **1976**, *18*, 1.

way, supports the above description of the cluster as a capped *closo*-species.

Cluster **3** follows the same geometry and electron count as **2**, and further corroborates the rationalization of the clusters as tetracapped trigonal prisms. The phenylacetylide ligand in this cluster is formally negatively charged, $[\text{PhCC}]^-$, and the overall charge of the cluster is 3^- instead of 2^- . The number of cluster-bonding electrons, however, is still 20 as in **2**. The calculated gap between the HOMO and the first cluster-based LUMO is also similar, 2.90 eV. The real HOMO–LUMO gap, however, is 2.16 eV because the LUMO and LUMO(+1) are the two lowest-lying π^* orbitals of the phenyl ring.

Finally, cluster **4** is also of the same overall geometry as that of **2** and **3** but carries an extra electron, 21 cluster-bonding electrons, and should be considered as a capped *intermediate* cluster. As already discussed, an *intermediate* cluster is a cluster with an electron count between those of *closo* and *nido* clusters, i.e., between 20 and 22, respectively. The half-occupied HOMO orbital for this cluster is exactly the same orbital that appears as a LUMO for **2** and LUMO(+2) for **3**. Furthermore, it is exactly the same frontier orbital that was described above for the empty Ge_9 clusters, i.e., bonding within the triangular bases of the trigonal prism but antibonding between them. It changes energy greatly upon changes in the lengths of the prismatic edges. Of course, the orbital in the NiL-capped clusters is perturbed by the contribution of the capping Ni-atom and by the opening of the capped triangular base (reduces bonding character), but its energy is most strongly affected by the lengths of the prismatic edges. Thus, this orbital has dropped in energy in **4** and carries the additional electron, and this correlates nicely with the longer prismatic edges in this cluster, 3.052(5), 3.220(4), and 3.250(4) Å, compared to 3.070(3) Å in **2** and to 3.1042(8), 3.1075(7), and 3.1366(8) Å in **3**. Energetically, exactly as in the empty Ge_9 clusters, the orbital is positioned in a gap and is well separated from the orbital above it with a HOMO–LUMO gap of 2.40 eV as well as from the orbital below it with a HOMO–HOMO(–1) gap of 1.23 eV.

The overall shape observed for clusters **2**, **3**, **4**, **6**, the two halves of the dimer $[(\text{Ni}@ \text{Ge}_9)\text{Ni}(\text{Ni}@ \text{Ge}_9)]^{4-}$, and the Pt-centered $[\text{Pt} @ (\text{Sn}_9\text{Pt} - \text{PPh}_3)]^{2-}$, has been observed before for a homoatomic cluster made of 10 indium atoms and centered by Ni, Pd, or Pt, $[\text{M}@ \text{In}_{10}]^{10-}$.¹⁸ The latter exist as isolated clusters in the Zintl phases $\text{K}_{10}\text{In}_{10}\text{M}$ made by high-temperature reactions from stoichiometric mixtures of the corresponding elements. The indium atom capping the triangular base of the tricapped trigonal prism is similarly “pulled” toward the central transition-metal atom and analogously causes expansion of the triangular prismatic base. The central atom plays the same role of providing orbitals (mainly the empty s and p) for overlap with appropriate cluster orbitals and thus improving the overall bonding within the cluster. Furthermore, with the exception of **4**, all clusters listed above are isoelectronic with these indium clusters. $[\text{M}@ \text{In}_{10}]^{10-}$ carries 20 cluster-bonding electrons that are provided by the 10 indium vertexes (each indium contributes one electron) and the charge of the cluster. Such geometric and electronic analogies are important because they can be used as a guide to search for other Ge–M clusters. Thus, in addition to $[\text{M}@ \text{In}_{10}]^{10-}$ with one capped triangular base, indium forms 11-atom empty clusters In_{11}^{7-} where both triangular bases of the

tricapped trigonal prism are capped and expanded.¹⁹ This cluster is hypoelectronic and carries 18 cluster-bonding electrons instead of the expected 20 for a bicapped *closo*-cluster (a capping atom does not change the number of electrons). The discrepancy is due to the distortions associated with the opening of the triangular bases and the compression of the two capping atoms toward the center of the cluster. This pushes to a higher energy a molecular orbital that is bonding within the capped triangular bases, but antibonding between them and the atoms that cap them. However, calculations show that for a centered cluster this molecular orbital is stabilized and filled making the cluster a 20-electron species, a hypothetical $[\text{Ni}@ \text{In}_{11}]^{9-}$. Continuing the analogy with Ge–Ni clusters, such a cluster would correspond to $[\text{Ni}@ \text{Ge}_9(\text{Ni}-\text{L})_2]^{2-}$ where both triangular bases of the tricapped trigonal prism of germanium are capped by Ni–L fragments. This and the fact that such clusters can fuse via the capping nickel atom as in $[(\text{Ni}@ \text{Ge}_9)\text{Ni}(\text{Ni}@ \text{Ge}_9)]^{4-}$ makes feasible eventual synthetic exploration for extended oligomeric units such as $[(\text{Ni}@ \text{Ge}_9)\text{Ni}(\text{Ni}@ \text{Ge}_9)\text{Ni}(\text{Ni}@ \text{Ge}_9)]^{6-}$ and even longer formations or infinite chains. Such species, in a way, will complement the existing oligomers and polymers of empty Ge_9 clusters, i.e., $[\text{Ge}_9 = \text{Ge}_9 = \text{Ge}_9]^{6-}$, $[\text{Ge}_9 = \text{Ge}_9 = \text{Ge}_9 = \text{Ge}_9]^{8-}$, and $\infty [-(\text{Ge}_9^{2-})-]$.

Experimental Section

General Data. All manipulations were carried out under an inert atmosphere using standard Schlenk-line and/or glovebox techniques. Ethylenediamine (Acros, 99%) was distilled over sodium metal, collected and redistilled over K_4Sn_9 and/or K_4Pb_9 intermetallics. The K_4Ge_9 precursor was synthesized from a stoichiometric mixture of the elements (K: 99+%, Strem; Ge: 99.999%, Alfa-Aesar) heated at 900 °C over 2 days in sealed niobium containers jacketed in evacuated fused-silica ampules. 2,2,2-crypt (Acros, 98%), $\text{Ni}(\text{PPh}_3)_2(\text{CO})_2$ (Strem, 98%), and $\text{Ni}(\text{COD})_2$ (Strem, 98+%), were used as received after carefully drying them under vacuum. Phenylacetylene (Aldrich, 98%) and KH (Acros) were used as received. KCCPh was synthesized by reaction of an ethylenediamine solution of phenylacetylene (1 mL, 0.009 mol) with a toluene suspension of KH (365 mg, 0.009 mol) which yielded a white powder after copious bubbling. The resulting solid was washed with toluene, dried under vacuum, and characterized as KCCPh. Electrospray mass spectra were recorded from DMF or ethylenediamine solutions (10–20 μM) on a Micromass Quattro-LC triple quadrupole mass spectrometer (125 °C source temperature, 150 °C desolvation temperature, 3 kV capillary voltage, and 25 V cone voltage). NMR spectra were recorded on a Varian UNITYplus 300 MHz spectrometer and referenced to an internal capillary containing TMS (10% in CD_3OD). IR spectra were recorded from ethylenediamine solutions of the corresponding crystalline products (under argon in a gastight cell, Perkin-Elmer Paragon 1000 FT-IR spectrometer).

$[\text{K}(\mathbf{2},\mathbf{2},\mathbf{2}\text{-crypt})]_3[\text{Ge}_9\text{Ni}-\text{CO}]$. K_4Ge_9 (92 mg, 0.114 mmol) and 2,2,2-crypt (153 mg, 0.406 mmol) were dissolved in ethylenediamine (3 mL) in a test tube inside a glovebox and allowed to stir for several minutes before addition of $\text{Ni}(\text{PPh}_3)_2(\text{CO})_2$ (146 mg, 0.228 mmol). The reaction mixture was stirred for 2 h after which the resulting dark-red/black solution was filtered and the black filtrate layered with toluene to allow for crystallization. Large, dark-red/brown block-shaped crystals suitable for X-ray diffraction were obtained after 2 days (45% crystalline yield). IR (en, cm^{-1}): 1820 (ν_{CO}).

$[\text{K}(\mathbf{2},\mathbf{2},\mathbf{2}\text{-crypt})]_2[\text{Ni} @ (\text{Ge}_9\text{Ni}-\text{CO})] \cdot \text{tol}$. K_4Ge_9 (98 mg, 0.121 mmol) and 2,2,2-crypt (150 mg, 0.398 mmol) were dissolved in ethylenediamine (3 mL) in a test tube inside a glovebox and allowed to stir for several minutes before addition of $\text{Ni}(\text{COD})_2$ (50 mg, 0.182

(18) Sevov, S. C.; Corbett, J. D. *J. Am. Chem. Soc.* **1993**, *115*, 9089.

(19) Sevov, S. C.; Corbett, J. D. *Inorg. Chem.* **1991**, *30*, 4875.

Table 1. Selected Data Collection and Refinement Parameters for (K-crypt)₃**1**, (K-crypt)₂**2**·tol, (K-crypt)₃**3**·en, and (K-crypt)₃[(**4**)_{0.735}(**5**·en)_{0.265}]·en

compound	(K-crypt) ₃ 1	(K-crypt) ₂ 2 ·tol	(K-crypt) ₃ 3 ·en	(K-crypt) ₃ [(4) _{0.735} (5 ·en) _{0.265}]·en
fw	1986.79	1722.05	2178.72	2122.14
space group, <i>Z</i>	<i>P</i> 2 ₁ /n, 4	<i>P</i> 6 ₃ /m, 2	<i>P</i> 1̄, 2	<i>P</i> 2 ₁ /n, 4
<i>a</i> (Å)	14.196(4)	11.9064(15)	14.6754(8)	17.254(3)
<i>b</i> (Å)	25.572(7)	11.9064(15)	15.2504(8)	23.182(4)
<i>c</i> (Å)	21.630(6)	25.724(7)	21.3415(12)	21.302(4)
α (deg)			82.578(3)	
β (deg)	97.731(5)		87.789(4)	96.909(4)
γ (deg)			69.499(3)	
<i>V</i> (Å ³)	7780(3)	3158.1(10)	4436.2(4)	8458(3)
ρ _{calc} (g·cm ⁻³)	1.696	1.811	1.631	1.667
radiation, λ (Å), temp (K)	Mo Kα, 0.71073, 100			
μ (cm ⁻¹)	3.885	4.985	3.619	3.740
R1/wR2, ^a <i>I</i> ≥ 2σ(<i>I</i>) (%)	5.98/14.07	6.54/16.32	4.92/11.40	6.19/13.69
R1/wR2, ^a all data (%)	6.70/14.29	7.11/16.59	6.25/11.89	11.74/15.29

^a R1 = [Σ||*F*_o| - |*F*_c||]/Σ|*F*_o|; wR2 = {[Σw[(*F*_o)² - (*F*_c)²]²]/[Σw(*F*_o)²]}^{1/2}; w = [σ²(*F*_o)² + (AP)² + BP]⁻¹, where *P* = [(*F*_o)² + 2(*F*_c)²]/3 and the *A* and *B* values are 0.0001 and 54.71 for (K-crypt)₃**1**, 0.0561 and 21.61 for (K-crypt)₂**2**·tol, 0.036 and 17.90 for (K-crypt)₃**3**·en, and 0.0745 and 0.00 for (K-crypt)₃[(**4**)_{0.735}(**5**·en)_{0.265}]·en, respectively.

mmol). The reaction mixture was allowed to stir for 1 h after which Ni(PPh₃)₂(CO)₂ (89 mg, 0.139 mmol) was added and the mixture stirred for an additional hour. The resulting dark-red/black solution was filtered, and the filtrate was layered with toluene. Large, red crystalline plates of [K(2,2,2-crypt)]₂[Ni@Ge₉Ni(CO)]·tol (53% crystalline yield) could be observed on the walls of the test tube after 1–2 day. IR (en, cm⁻¹): 1930 (ν_{CO}). The same compound was also crystallized from pyridine and DMF solutions layered with toluene.

[K(2,2,2-crypt)]₃[Ni@(Ge₉Ni-C≡CPh)]·en. A crystalline sample of [K(2,2,2-crypt)]₂[Ni@Ge₉Ni(CO)] (160 mg, 0.098 mmol) was dissolved in ethylenediamine (3 mL) in a test tube inside a glovebox and allowed to stir for 5–10 min. Added to the resulting dark-red/black solution were potassium phenylacetylide (27 mg, 0.196 mmol) and 2,2,2-crypt (74 mg, 0.196 mmol), and the mixture was allowed to stir for 3 h. The reaction mixture was filtered, and the filtrate was layered with toluene. Large black crystals of [K(2,2,2-crypt)]₃[Ni@Ge₉Ni(C≡CPh)]·en (52% crystalline yield) suitable for X-ray diffraction were obtained after several weeks. IR (en, cm⁻¹): 1933 (ν_{C≡C}). ¹³C{¹H} (en, TMS internal reference): δ 138.7 (s, *i*-C₆H₅), 132.5 (s, *o*-C₆H₅), 129.9 (s, *p*-C₆H₅), 129.2 (s, *m*-C₆H₅), 127.9 (s, -C≡), 126.3 (s, ≡C-H).

[K(2,2,2-crypt)]₃{[Ni@(Ge₉Ni-en)]_{0.735}[(Ni@Ge₉)_{0.265}]·en. K₄Ge₉ (87 mg, 0.107 mmol) and 2,2,2-crypt (122 mg, 0.324 mmol) were dissolved in ethylenediamine (3 mL) in a test tube inside a glovebox and allowed to stir for several minutes before addition of Ni(COD)₂ (64 mg, 0.232 mmol). The reaction mixture was stirred for 2 h after which the resulting dark-red/brown solution was filtered, and the black filtrate was layered with toluene to allow for crystallization. Large, bright-red platelike crystals of the compound (20% crystalline yield) suitable for X-ray diffraction were obtained after 2 days.

Crystallographic studies. Data sets were collected on a Bruker APEX diffractometer with a CCD area detector at 100 K with Mo Kα

radiation. The crystals were selected under Paratone-N oil, mounted on fibers, and positioned in the cold stream of the diffractometer. The structures were solved by direct methods and refined on *F*² using the SHELXTL v5.1 package (after absorption corrections with SADABS). Details of the data collections and refinements are given in Table 1. Specifics of the four structures are discussed in the Results section.

Computational Methods. Single-point DFT calculations were performed on all clusters employing the atomic positions as elucidated from single-crystal X-ray diffraction data. Becke 3-parameter density functional with Lee–Yang–Parr correlation (B3LYP)²⁰ and restricted open-shell Hartree–Fock wave functions in conjunction with a 6-31++g* basis set were used. The computations were executed with the Gaussian 98 package, revision A.11.3,²¹ on Notre Dame’s “Bunch-o-Boxes” Beowulf cluster.

Acknowledgment. We thank the National Science Foundation (CHE-0446131) for the financial support of this research and for the purchase of the Bruker APEX diffractometer (CHE-0443233) and the “Bunch-o-Boxes” cluster (DMR-0079647).

Supporting Information Available: X-ray crystallographic file in CIF format (four structures), drawings of the four clusters with anisotropic displacement ellipsoids, drawings of the observed disorder and overlap of clusters, closer view of the mass spectrometry of **2**, and complete ref 21. This material is available free of charge via the Internet at <http://pubs.acs.org>.

JA058652G

- (20) (a) Becke, A. D. *J. Chem. Phys.* **1993**, *98*, 5648. (b) Lee, C. T.; Yang, W. T.; Parr, R. G. *Phys. Rev. B* **1988**, *37*, 785.
 (21) Frisch, M. J.; et al. *Gaussian98*, revision A.11.3; Gaussian, Inc.: Pittsburgh, PA, 2002.